# Intensity-dependent phase-matching effects in harmonic generation

**J. Peatross**

*General Physics Institute, Russian Academy of Sciences, 38 Vavilov Street, 117942 Moscow, Russia, and Department of Physics and Astronomy, University of Rochester, Rochester, New York 14627*

**M. V. Fedorov**

*General Physics Institute, Russian Academy of Sciences, 38 Vavilov Street, 117942 Moscow, Russia*

**K. C. Kulander**

*Department of Physics, Lawrence Livermore National Laboratory, Livermore, California 94551, and Joint Institute for Laboratory Astrophysics, University of Colorado, Boulder, Boulder, Colorado 80309*

Received August 8, 1994

In high-order harmonic generation by an intense laser, intrinsic phases can develop at the atomic level between the laser field and the individual emitted harmonics. Because intrinsic phases can vary rapidly with the laser intensity, they can strongly influence phase matching to the extent that the laser intensity varies within the generating medium. Previously reported measurements of broad far-field harmonic emission patterns as well as measured asymmetries in the emission with respect to the axial positioning of the medium in the focus can be explained by intrinsic phases. An experimental method for further study of intrinsic phases is proposed that involves harmonic generation in two counterpropagating laser beams. The periodic intensity modulation created by the two beams coupled with the intensity-dependent intrinsic phases allows harmonic light to propagate in directions with otherwise extremely poor phase-matching conditions.

## 1. INTRODUCTION

High-order harmonic generation by a strong laser field in a gaseous medium is a highly nonlinear process. An interesting phenomenon associated with high-order harmonic generation is the development of intrinsic phase variations at the atomic level between the phase of the laser field and the phases of the individual emitted harmonics. These phase variations occur most prominently in the intensity range of the harmonic plateau, where many harmonic orders are generated with approximately the same conversion efficiency. Many theoretical models[1–6] that describe the atomic dipole response to a strong laser field inherently contain marked intensity dependences of these intrinsic phases that differ with harmonic order, although this fact has received little attention in the literature. In this paper we investigate the effects of intensity-dependent phases on the overall phase matching of harmonic generation in a laser focus where the intensity varies spatially.

The dipole response of Xe, which has been calculated for a 1.064-$\mu$m laser field by numerical integration of the Schrödinger equation in three dimensions, and which has been reported on in the literature,[7–10] shows strong dependences of the harmonic phases on the laser intensity. (Again, the phases were not emphasized previously.) Figure 1(a) shows the square amplitude of the calculated 13th-harmonic component of the dipole oscillation as a function of laser intensity. Figure 1(b) shows the amplitude of the same data plotted in polar coordinates where the azimuthal coordinate is the phase of the harmonic. Along the curve, the laser intensity continually increases from the center outward. The filled squares in both plots correspond to calculated points, and the connecting curves were determined from a cubic spline of the dipole harmonic amplitude in complex notation as a function of the laser field amplitude. The spline provides the smoothest possible connection of the points; if the further points were to be calculated they might well deviate from these connecting curves. Although it is not easily seen in the figure, the curve spirals outward in the clockwise direction with only momentary setbacks to an ever-decreasing phase [more easily seen in Fig. 3(a) below]. The calculations of the other harmonic orders generated in Xe, orders up to the 33rd, show similar behavior. In this paper we use the calculation of the 13th-harmonic dipole response in Xe to represent the behavior of high-order harmonic emission in general. It may be expected that the phase-matching calculations presented in this paper would remain qualitatively similar if they were instead based on any of a number of models.[1–6]

Recently, experimental conditions were created in which the harmonics could be thought of as emerging from a single plane in the laser focus rather than from a three-dimensional volume.[11,12] The very long focusing geometry and the low gas density minimized geometrical and refractive phase mismatches so that the harmonic far-field angular distributions could be more directly associated with the atomic response to the radial laser intensity distribution in the focus. The appearance of

0740-3224/95/050863-08$06.00 ©1995 Optical Society of America

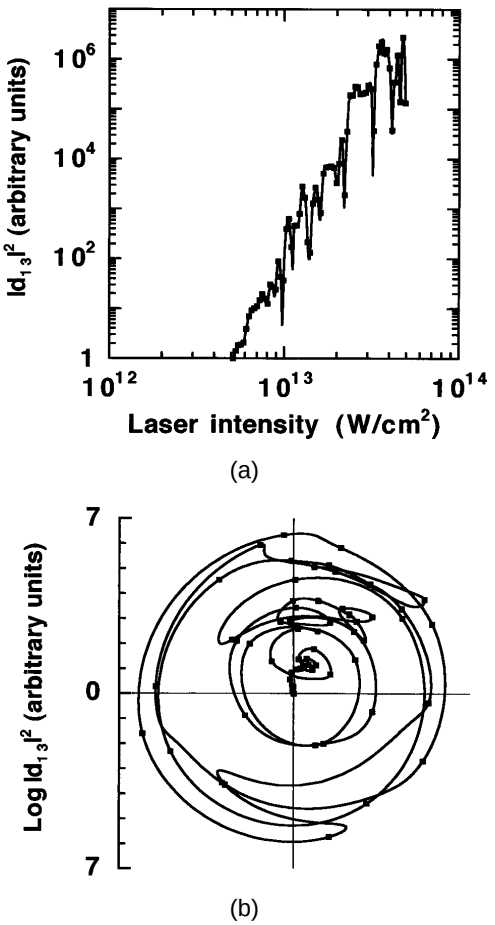


Fig. 1. (a) Single-atom response for the 13th harmonic generated in Xe plotted as a function of laser intensity. (b) Single-atom response for the 13th harmonic generated in Xe plotted in a polar format where the azimuthal coordinate corresponds to the phase of harmonic emission relative to the laser's phase.

broad wings in the harmonic far-field angular profiles under such conditions indicates the presence of strong intensity-dependent intrinsic phases, in agreement with the theoretical models. In other experiments performed by Balcou and L'Huillier,[13] observations were made that suggested the presence of intensity-dependent phases, in the case brought about by axial changes of the laser intensity within the generating medium.

## 2. RADIAL INTERFERENCES FROM INTENSITY-DEPENDENT PHASES

From the experimental results of Refs. 11 and 12 it was determined that the phase of high harmonic emission has a strong dependence on the laser intensity. The conclusion is based on an observation of the far-field angular profiles of high-order harmonics emitted from a laser focused into various noble gases. The measurements differ from similar measurements[14–16] in which harmonics of typically higher order were investigated with tighter-focused geometries and at higher gas pressures and for which the far-field patterns have been explained in terms of geometric and refractive phase mismatches. In contrast, in the experiments of Refs. 11 and 12 geometric and refractive phase mismatches were minimized, and the harmonics can be understood as coming from a plane at the laser focus. Under these conditions the far-field patterns of the harmonics are seen to have broad structures with widths approximately equal to the width of the emerging laser profile.

Because high-order harmonics have wavelengths much shorter than the laser wavelength, the broad features in their far-field patterns imply either that the harmonics are generated in an extremely small area or else that they have strong phase variations across their wave fronts as they emerge from the focus. The first possibility is dismissed because it implies that harmonic production rates have extremely sharp dependences on the laser intensity instead of the gradual dependences that have been observed in the intensity range where the harmonic plateau appears.[4,9,17] For example, in the absence of phase variations the emitting region of the $q$th harmonic in the focus must be $q$ times narrower than the laser distribution in order for its far-field pattern to have the same width as the emerging laser, and this implies a harmonic production law that follows the laser intensity raised to the extraordinarily high power of $q^2$, assuming a Gaussian laser distribution. The remaining possibility, phase variations across the individual harmonic wave fronts, which may arise from a variety of effects, can be associated with the radially varying laser intensity in the case of the experiments of Refs. 11 and 12 because other possible sources of phase inhomogeneities were excluded by experimental design.

Consider harmonic emission from a single atom. The $q$th-harmonic component of the field emitted from an atom stimulated by a laser can be written as[18]

$$E_q(\mathbf{r}, t + r/c) = -\frac{{k_q}^2}{8\pi\epsilon_0 r}\exp(-iq\omega t)|d_q[I_L(t)]| \times \exp\{i\phi_q[I_L(t)] + iq\phi_L\} + \text{c.c.}, \quad (1)$$

where $d_q$ is the amplitude of the $q$th-harmonic component of the atomic dipole, $I_L$ is the laser intensity, $\omega$ is the laser frequency, $k_q \cong qk$ is the $q$th-harmonic wave number, $\phi_L$ is the phase of the laser at the atom, and $\phi_q$ is the atomic intrinsic phase, which depends on the laser intensity. It has been assumed that $\mathbf{r}$ points in a direction very nearly perpendicular to the dipole moment vector. Implicit in this formulation is an adiabatic assumption in which the details of the past history of the laser pulse are not important.

When more than one atom is present we may sum over the emission of the individual atoms if it is assumed that each atom is not influenced by emission from neighboring atoms. Consider emission from a collection of atoms lying in the plane of a laser focus. The component of the electric field that oscillates with the frequency of the $q$th harmonic in the far-field zone (Fraunhofer approximation) is[19]

$$E_q(\mathbf{r}, t + r/c) = \frac{{k_q}^2 N_0}{4\epsilon_0 r}\exp(-iq\omega t)\int_0^\infty \mathrm{d}\rho'\rho' J_0\left(\frac{k_q\rho\rho'}{z}\right) \times |d_q[I_L(\rho', t)]|\exp\{i\phi_q[I_L(\rho', t)] + iq\phi_L\} + \text{c.c.}, \quad (2)$$

where we have assumed azimuthal symmetry and have performed the angular integration that gives rise to the

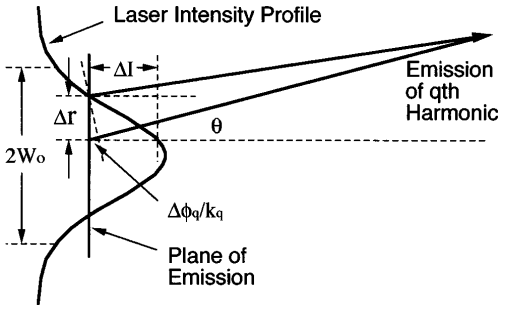


Fig. 2. Schematic depicting how an intensity-dependent phase variation of the $q$th-harmonic emission can cause the harmonic light to scatter into angles off axis. A change of $\Delta r$ in radius corresponds to a change of $\Delta I$ in laser intensity. The associated change in the harmonic phase $\Delta\phi_q$ causes the light to scatter into an angle $\theta \sim \Delta\phi_q/(k_q \Delta r)$.

zeroth-order Bessel function. We have employed cylindrical coordinates where $r = \sqrt{\rho^2 + z^2}$, and the atomic distribution has been chosen to lie in the plane $z = 0$. $N_0$ is the area density of atoms, which we take to be constant. Equation (2) is the spatial Fourier transform (or Hankel transform) of the $q$th-harmonic emission distribution in the laser focus. For a Gaussian laser the intensity in the plane of the focus is given by[20]

$$I_L(\rho', t) = I_0 \exp\left(-\frac{2\rho'^2}{w_0^2} - \frac{t^2}{\tau^2}\right), \tag{3}$$

where $w_0 = 2\lambda f^{\#}/\pi$ is the laser beam waist. In the plane of the laser focus we have $\phi_L = 0$.

The intrinsic phase $\phi_q$ can cause the harmonics to scatter into the broad angles observed in the experiments because of its radial dependence. Figure 2 shows a schematic of the scattering process that arises from this phase. The laser intensity translates into a radial phase variation of the $q$th harmonic according to the nature of $\phi_q$. The rate at which the intrinsic phase of the $q$th-harmonic emission changes with radius in the laser focus can be roughly estimated from

$$\Delta\phi_q/\Delta r \sim k_q \theta\,, \tag{4}$$

where $\theta \equiv \rho/z$ is the angle from the laser axis through which the far-field distribution extends.

For the experiments of Refs. 11 and 12, harmonics of 1.054-$\mu$m light with orders in the mid 30's and below were seen to emerge with angles as wide as 10 mrad from the laser axis. Estimate (4) gives for the 13th harmonic $\Delta\phi_{13}/\Delta r \sim 0.25\pi\ \mu\text{m}^{-1}$, which implies a phase change of $\pi$ over a radial distance of only 4 $\mu$m, one fifteenth of the laser focal radius $w_0 = 60\ \mu$m ($1/e^2$ intensity point). Over the distance 4 $\mu$m, the laser intensity varies at most by 8%. It is implied not that the phase must vary with this rate at all intensities but only that it varies with at least this rate at some intensities. This turns out to be a conservative estimate in view of Fig. 1, and we will comment on this further in Section 3.

Figure 3(a) shows the square amplitude and phase of the 13th-harmonic component of the Xe dipole plotted as a function of radius in a Gaussian laser profile with peak intensity $4.5 \times 10^{13}$ W/cm$^2$. This is based on the same numerical data of Refs. 7–10 as shown in Fig. 1. As we mentioned above, the phase tends to decrease continually with increasing intensity. Figure 3(b) shows the far-field intensity profile calculated from Eq. (2) by use of the focal emission distribution of Fig. 3(a). The intensity profile corresponds to an instant in time when the laser intensity in the focus is at $4.5 \times 10^{13}$ W/cm$^2$. The dotted curve is a repeat of the calculation with the intrinsic phase $\phi_{13}$ held constant. With this phase excluded, the far-field pattern becomes much brighter and concentrates near the laser axis with little evidence of wings. Nevertheless, the total emitted light is the same in the two cases, as can easily be proved by application of Parseval's theorem to the Fourier transform involved in finding the far-field pattern [Eq. (2)]. The azimuthal symmetry means that the portions of the distribution that are farther from the axis carry more energy (proportional to $\theta$). In fact, with the phase included, much of the energy is scattered into angles beyond those shown in Fig. 3(b); the central structure has only ~10% of the energy. It should be noted,

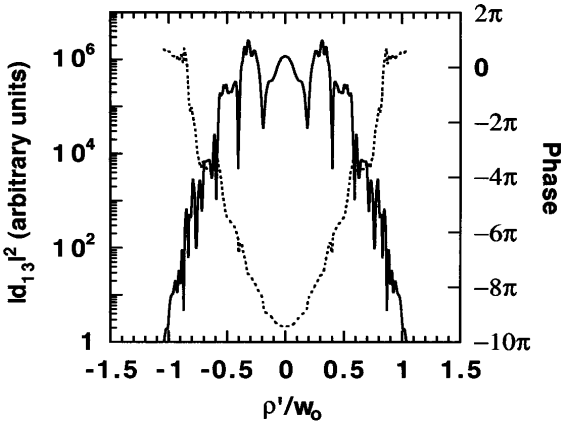


(a)

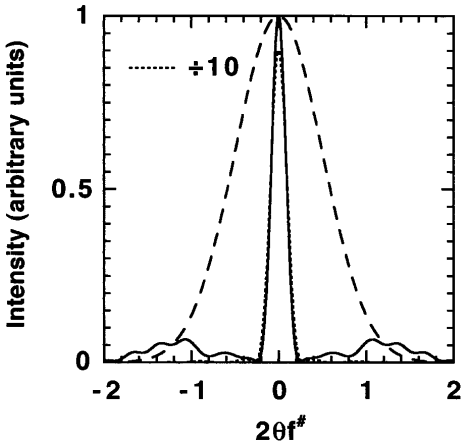


(b)

Fig. 3. (a) Single-atom response for the 13th harmonic generated in Xe plotted as a function of radius in a Gaussian laser focus with peak intensity $4.5 \times 10^{13}$ W/cm$^2$ (solid curve). The dotted curve is the phase of harmonic emission relative to the laser's phase indicated on the right vertical axis. (b) Far-field intensity distribution calculated from the planar emission distribution of (a). The dotted curve is a repeat of the calculation performed with the intrinsic phase held constant. The dotted curve has been divided by a factor of 10. The dashed curve depicts the laser intensity profile. The units on the horizontal axis can also be written as $\rho/w(z)$, where $w(z) \cong w_0 z/z_0$.

however, that the total emitted energy need not be conserved with a change in the intrinsic phase if we consider emission from a volume for which the far-field pattern is not simply a Fourier transform of a planar distribution.

It might be asked whether the lack of harmonic emission from the center of the focus in the case of strong ionization of the medium (ignoring the refractive index) might be sufficient to cause broad wings in the far-field pattern in the absence of intensity-dependent phases. The answer is no because the lack of emission in a region affects the far-field pattern no more profoundly than does the jagged shape of the solid curve in Fig. 3(a). If emission is excluded from a region in the center of the focus, the far-field pattern remains similar to the dotted curve in Fig. 3(b) when $\phi_q$ is held constant.

## 3. FINITE THICKNESS OF THE INTERACTION REGION

We may extend the formulation of Eq. (2) to describe emission from a three-dimensional volume in the laser focus. This involves an additional integral in the $z$ direction. The component of the electric field that oscillates with the frequency of the $q$th harmonic, again in the far field, is[9,10,12,13]

$$E_q(\mathbf{r}, t + r/c) = \frac{k_q{}^2 N_0}{4\epsilon_0 r} \exp(-iq\omega t) \int_{z_1}^{z_2} \mathrm{d}z' \int_0^\infty \mathrm{d}\rho' \rho' J_0\left(\frac{k_q \rho \rho'}{z}\right) \times |d_q[I_L(\rho', z', t)]| \times \exp\left\{ i\phi_q[I_L(\rho', z', t)] + iq\phi_L(\rho', z') + i\frac{k_q \rho^2 z'}{2z^2} \right\} + \text{c.c.} \tag{5}$$

In this case, $N_0$ is the volume atomic density, which we have taken to be a constant for $z_1 \le z' \le z_2$ and zero elsewhere. Equations (2) and (5) are similar in form except for the term $k_q \rho^2 z'/2z^2$, which is a phase mismatch that occurs because of the thickness of the medium when the harmonic light propagates to points off axis in the far field. Near the focus, the Gaussian laser intensity envelope may be written as[20]

$$I_L(\rho', z', t) = \frac{I_0}{1 + z'^2/z_0{}^2} \times \exp\left[ -\frac{2\rho'^2}{w_0{}^2(1 + z'^2/z_0{}^2)} - \left(\frac{t - z'/c}{\tau}\right)^2 \right], \tag{6}$$

and the local phase of the laser field written as

$$\phi_L(\rho', z') = k_L \rho'^2/2R(z') - \tan^{-1}(z'/z_0) - \int_{-\infty}^{z'} \mathrm{d}z'' \Delta k(z'')/q\,, \tag{7}$$

where $z_0 = \pi w_0{}^2/\lambda$ is the Rayleigh range. The first term in the phase of the laser field $\phi_L(\rho', z')$ is associated with the radius of curvature of the laser wave front $R(z') = z' + z_0{}^2/z'$, the second term is the Gouy shift, and the final term arises as a result of the phase mismatch of the optical index $\Delta k = k_q - qk$. Significant ionization introduces in both $\Delta k$ and $N_0$ additional $\rho'$, $z'$, and $t$ dependences because of atomic depletion and the refractive effects of free electrons. The latter can also affect the propagation of the incident beam. In the present paper we consider only short pulse durations ($\tau \le 1$ ps) and low gas density ($N_0 \le 3 \times 10^{16}$ cm$^{-3}$ $\sim$ 1 Torr) so that $\Delta k$ may be taken to be zero and $N_0$ constant.

Figure 4 shows the far-field profile of the 13th harmonic similar to that of Fig. 3(b), except that it is calculated from Eq. (5) assuming emission from a volume centered at the origin with thickness $z_0/5$ (one tenth of the confocal parameter). This is approximately the experimental condition of Refs. 11 and 12. Except for a slight diminution in the signal away from the axis center, the distribution looks the same as that from a plane [Fig. 3(b)]. This is in agreement with the claim made in Refs. 11 and 12 that the experimental conditions allow the harmonics to be thought of as emerging from a plane. In typical high-harmonic generation experiments the accumulated energy of individual harmonics is measured for an entire laser pulse. The dotted curve is the calculated far-field accumulated energy pattern for the same conditions as for the solid curve. Each point is obtained by integration of the emission harmonic intensity over a temporally Gaussian laser pulse with peak intensity $4.5 \times 10^{13}$ W/cm$^2$. As the laser intensity changes, the radial distribution of intrinsic phases in the laser focus changes so that the features in the harmonic far-field emission pattern evolve and shift position with time. Thus the more-defined features seen in the snapshot are smoothed out. Figure 4 is in good agreement with the far-field patterns measured in Refs. 11 and 12.

The approximation that the harmonics emerge from a plane becomes less valid for angles in the far field away from the axis. When this happens the interpretation of Eq. (4) must be altered because the thickness of the generating medium becomes important. Figure 5 shows a schematic depicting the phase error introduced by the medium thickness when harmonics propagate into angles off axis. It is this effect that degrades the emission at the wide angles in Fig. 4. Harmonic light emitted from the beginning and the end of the medium follows separate paths with a length difference of $l\theta^2/2$, where $l$ is the

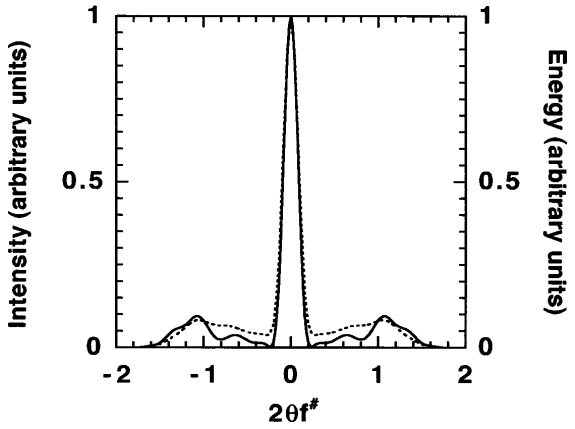


Fig. 4. Far-field intensity distribution of the 13th harmonic generated in a medium of thickness $z_0/5$ centered in a laser focus with peak intensity $4.5 \times 10^{13}$ W/cm$^2$ (solid curve). The dotted curve is a repeat of the calculation in which the temporal integration over a Gaussian laser pulse has been performed to yield the accumulated energy as indicated on the right vertical axis.

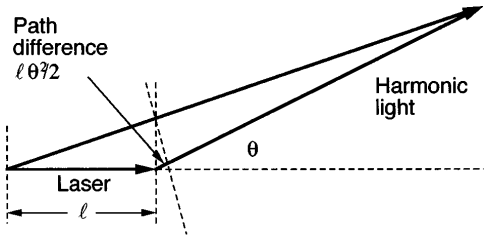


Fig. 5. Schematic showing the phase error that occurs as a result of the thickness of the generating medium when the harmonics emerge into angles off the laser axis.

thickness of the medium. A phase difference of $\pi$ occurs at an angle $\theta \sim \sqrt{2\pi/k_q l}$. At greater angles the phase difference increases beyond $\pi$, but this does not necessarily mean a resurgence in the signal because all locations between the beginning and the end of the medium emit with varying degrees of phase error. In the experiments of Refs. 11 and 12 the gas target thickness was 1 mm, which causes a phase difference of $\pi$ when the 13th harmonic is directed off axis by 9 mrad, approximately the maximum angle for which signal was observed. Thus, if the harmonic light were scattered by very abrupt radial phase changes arises from the atomic dipole, say, from sudden slips of $\pi$ as might occur for resonance structures, the thickness of the medium would have prevented the light from scattering into the extremely wide angles implied by Eq. (4).

Figure 6 shows the same calculation of the far-field pattern as the solid curve in Fig. 4, except that the thickness of the active medium was increased to $z_2 - z_1 = z_0$ (one half of the confocal parameter). The laser intensity in the center of the focus was again assumed to be $4.5 \times 10^{13}$ W/cm$^2$, and no temporal integration was included. If the intensity profile were to be temporally integrated over a laser pulse as in the calculation for the dotted curve in Fig. 4, the many bumps would be smoothed out as the pattern evolved in time. As is evident, the angular structure of the far-field pattern is radically different from that of Fig. 4. This to a large degree is due to geometric phase mismatches[12,17] caused by the phase terms $\phi_L(\rho', z')$ and $k_q\rho^2 z'/2z^2$ in Eq. (5). Geometric phase mismatches within the laser focus have been described by L'Huillier *et al.*[10,21] Because of the medium's thickness, the interpretation of harmonic emission from a plane fails, and the estimate of Eq. (4) can no longer be used. The pattern in Fig. 6 is no brighter than the pattern in Fig. 4 (normalized in the same way) even though the medium is five times thicker. The dotted curve is a repeat of the calculation in which the intrinsic phase $\phi_{13}$ has been held constant. The radical change in the pattern shows that intensity-dependent phases remain important even in the presence of strong geometrical phase mismatches, although their effects become intermingled.

## 4. AXIAL INTERFERENCES FROM INTENSITY-DEPENDENT PHASES

If the harmonic-generating medium is thick enough, the laser intensity can significantly vary along its axis within the medium, and intensity-dependent phases can vary axially as well as radially. Experimental observations by Balcou and L'Huillier[13] showed that the intensities of individual harmonics generated with a tight focusing geometry (i.e., the generating medium's thickness approximately the same as the confocal parameter) are strongly dependent on the longitudinal position of the laser focus with respect to the gas distribution. The strong dependence on position was explained primarily through phase-matching geometry by which the harmonic production is expected to be symmetric with respect to the longitudinal position of the laser focus relative to the gas distribution. However, their data showed strong asymmetries. Although other possible explanations for the asymmetries were not ruled out (absorption, gas jets nonuniformity), they suggested that an intrinsic phase may be responsible. Under these conditions, axial phase variations of the atomic dipole response influence the phase matching.

Figure 7 shows the far-field on-axis intensity of the emitted 13th harmonic as a function of longitudinal position of the generating medium (solid curve). The thick-

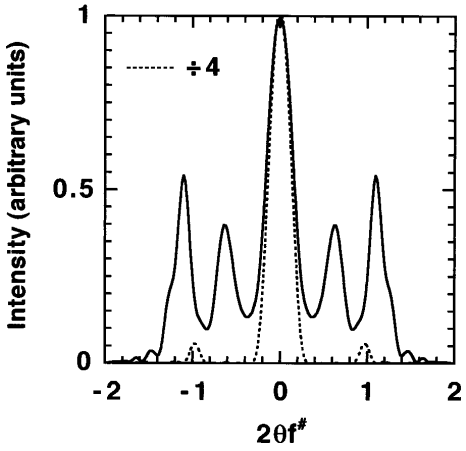


Fig. 6. Far-field intensity distribution corresponding to emission of the 13th harmonic generated in a medium of thickness $z_0$ centered in a laser focus with peak intensity $4.5 \times 10^{13}$ W/cm$^2$ (solid curve). The dotted curve is a repeat of the calculation performed with the intrinsic phase held constant. The dotted curve has been divided by a factor of 4.

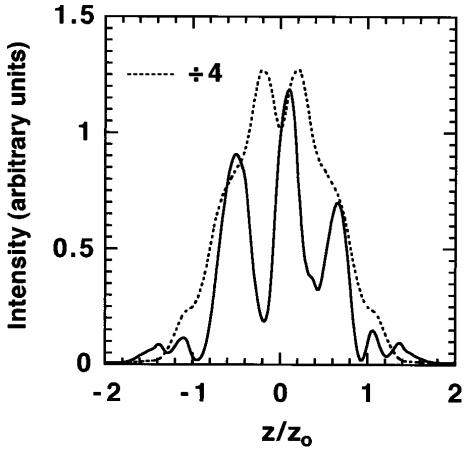


Fig. 7. Far-field axial intensity of the 13th-harmonic emission as a function of the longitudinal position of the gas distribution in the laser focus. The dotted curve is a repeat of the calculation performed with the relative phase held constant. The dotted curve has been divided by a factor of 4.

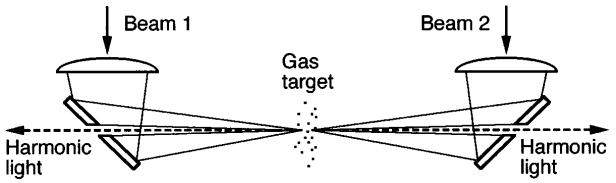


Fig. 8. Proposed experimental setup for studying intensity-dependent intrinsic phases. Harmonics are generated in counterpropagating beams focused off mirrors with holes in their centers.

ness of the medium was fixed at $z_2 - z_1 = z_0$, the same as for Fig. 6, and the center of the medium $(z_1 + z_2)/2$ was varied. We chose to examine the on-axis intensity of the harmonic in the far field rather than the energy in the entire angular pattern because the spectrometer used in the experiments of Balcou and L'Huillier accepted a cone angle of harmonic light much narrower than the laser beam.[22] However, a direct comparison cannot be made with their data because we did not include the temporal integration of the intensity and we used a square medium distribution, which has different geometric phase-matching properties from a smoother gas-jet profile. However, the asymmetry in the curve is qualitatively similar to the asymmetries observed in the experiments. The dotted curve is a repeat of the calculation with the intrinsic phase held constant. Aside from an overall increase in the harmonic intensity, the absence of the phase causes the details of the pattern to shift and to become symmetric. Thus the intrinsic phase variations that are due to an axially varying laser intensity are seen to influence harmonic production significantly and likely play a role in explaining the asymmetries in the data. Figures 4, 6, and 7 are all normalized in the same way so that their heights can be compared directly.

## 5. PHASE MATCHING IN COUNTERPROPAGATING BEAMS

A recent technique[23] for separating harmonic light from the laser beam allows for a new method of examining intrinsic phases. With this technique it is possible to observe harmonics generated in two counterpropagating laser beams. Figure 8 shows a schematic of a proposed experimental setup that uses mirrors with holes in them. When the two annular beams are focused into the generating medium the holes in the beam centers fill in to produce a central peak similar to that of a usual laser focus surrounded by faint rings. Because of the nonlinearity of high-order harmonic generation, the harmonics are emitted primarily from the central peak, and they emerge as usual, centered along the laser axis so that much of their energy lies inside the holes. The holes are necessary because of the lack of suitable materials able to transmit the vacuum ultraviolet.

The counterpropagating beams produce a periodic intensity variation throughout the laser focus that is ideal for the study of intensity-dependent intrinsic phases. In particular, the situation of one strong beam and one weak beam is interesting because, in the absence of intensity-dependent phases, phase matching for harmonic generation in the direction of the weak beam is extremely poor. However, when intensity-dependent phases are present, significant harmonic emission in the direction of the weak beam is possible, and the strength of the emitted light depends sensitively on the nature of the phases. This can occur even when the intensity of the weak beam is far too low to generate high-order harmonics alone.

Consider a small region and a brief time interval in the focus of two counterpropagating laser beams with local field strengths $E_1$ and $E_2$. The total field in this neighborhood can be approximated as the sum of two plane waves:

$$E_t(z, t) = \frac{E_1}{2} \exp(-i\omega t + ikz) + \frac{E_2}{2} \exp(-i\omega t - ikz) + \text{c.c.} \tag{8}$$

The two counterpropagating fields produce a stationary periodic intensity modulation described by

$$I_t(z) = I_1[(1 - \sqrt{I_2/I_1})^2 + 4\sqrt{I_2/I_1} \cos^2 kz]. \tag{9}$$

The maximum and minimum intensities of the periodic structure are $I_1(1 \pm \sqrt{I_2/I_1})^2$. Even when one field is much weaker than the other, say, $I_2 = I_1/100$, the intensity variation of the combined field can be rather high, more than 30%. When the fields are of unequal amplitude (assume $E_1$ larger than $E_2$) there is net propagation of the field in the direction of the stronger beam. The phase of this propagating field is $\omega t - kz + \Phi(z)$, where $\Phi(z)$ is a periodic phase distortion that goes to zero when $E_2$ is zero. The phase distortion can be written in the interval $[-\pi/2 \geq kz - n\pi \geq \pi/2]$ as

$$\Phi(z) = kz - \tan^{-1}\left(\frac{1 - \sqrt{I_2/I_1}}{1 + \sqrt{I_2/I_1}} \tan kz\right) - n\pi, \tag{10}$$

where $n$ is an integer.

The phase distortion $\Phi(z)$ introduces a microscopic phase mismatch for harmonic generation that is periodic over the interval $\lambda/2$. The total intensity is also periodic with this interval, so one can determine an effective dipole emission by considering phase matching over this length. The effective dipole emission in the direction of beam 1 is

$$d_q^{\text{Eff}}(I_1, I_2) = \frac{2}{\lambda} \int_{-\lambda/4}^{\lambda/4} \mathrm{d}z |\mathrm{d}_q\{I_t(z)\}| \times \exp\{i\phi_q\{I_t(z)\} + iq\Phi(z)\}. \tag{11}$$

Both phase terms $\phi_q\{I_t(z)\}$ and $\Phi(z)$ tend to degrade the emission according to how they vary over the interval. One can obtain the effective dipole emission in the direction of beam 2 from Eq. (11) by interchanging the limits of integration and the positions of $I_1$ and $I_2$ in Eq. (10). In this case, $\Phi(z)$ tends to suppress harmonic emission very sharply because it varies much more rapidly. However the intensity-dependent phase $\phi_q\{I_t(z)\}$ can compensate in part for the extremely poor phase matching in the direction of beam 2. The effective dipole emission of Eq. (11) can be used to calculate the macroscopic phase matching of the entire laser focus in the usual way by use of Eq. (5). However, the calculation is complicated by the fact that the individual local intensity of each beam must be considered at each place and time in the focus.

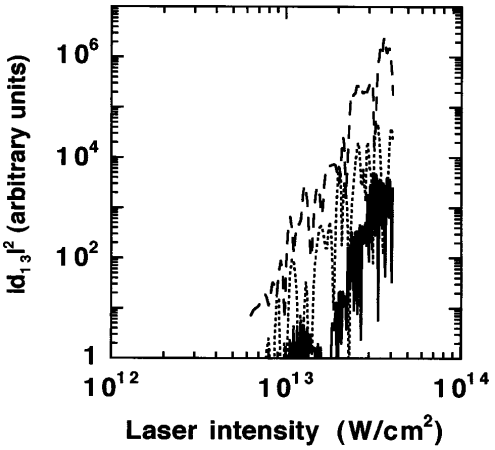


Fig. 9. Effective emission for the 13th harmonic in the direction of the weak beam when two beams of intensities $I_1$ and $I_2 = I_1/100$ are counterpropagated (solid curve). The dotted curve is the effective emission in the direction of the strong beam. The dashed curve is the single-atom response identical to that shown in Fig. 1(a).

Figure 9 shows the effective dipole emission for the 13th harmonic in the two directions as a function of $I_1$, where $I_2$ is held at $I_2 = I_1/100$. The solid curve (rapidly fluctuating) is the effective emission in the direction of beam 2. The dotted curve is the emission in the direction of beam 1. The dashed curve is the usual single-beam emission curve (valid for $I_2 = 0$). If the intensity-dependent phase $\phi_{13}$ is held constant, then the effective emission in the direction of beam 2 drops by more than 10 orders of magnitude and the emission in the direction of beam 1 increases to be close to that of the single-beam emission curve. One may also use this experimental arrangement using two beams to study the dependence of the intrinsic phases on laser polarization ellipticity by varying the polarization of one of the beams.

## 6. CONCLUSION

Intrinsic phases play a major role in high-order harmonic generation phase matching. They also strongly influence the coherence of the emerging harmonic beams inasmuch as the resulting interferences cause the light to scatter into wide angles where the various structures involve different phases. In the quest to find ways to increase harmonic conversion efficiency by improving phase-matching conditions, intrinsic phases will have to be considered. To this end, it may be possible to find situations in which intrinsic phases can be played against geometrical phase mismatches in order to improve over all phase matching. To do this, we must learn much more about the intrinsic phases.

## ACKNOWLEDGMENTS

We acknowledge the contribution of K. J. Schafer in the calculations of the harmonic dipoles. J. Peatross acknowledges previous work carried out jointly with D. D. Meyerhofer at the Laboratory for Laser Energetics, University of Rochester, which led to the present work. This research was supported in part by the National Science Foundation through the Program for Long- and Medium-Term Research at Foreign Centers of Excellence under contract INT-9302168. This research was also carried out in part under the auspices of the U.S. Department of Energy under contract W-7405-ENG 48. K. C. Kulander acknowledges the kind hospitality of the Joint Institute for Laboratory Astrophysics, University of Colorado, Boulder.

## REFERENCES

1. W. Becker, S. Long, and J. K. McIver, "Higher-harmonic production in a model atom with short-range potential," Phys. Rev. A **41,** 4112–4115 (1990).
2. B. Sundaram and P. W. Milonni, "High-order harmonic generation: simplified model and relevance of single-atom theories to experiment," Phys. Rev. A **41,** 6571–6573 (1990).
3. L. Plaja and L. Roso-Franco, "Adiabatic theory for high-order harmonic generation in a two-level atom," J. Opt. Soc. Am. B **9,** 2210–2213 (1992).
4. A. L'Huillier, L. A. Lompre, G. Mainfray, and C. Manus, "Multiple harmonic conversion in rare gases in strong laser fields," in *Proceedings of the 5th International Conference on Multiphoton Processes*, G. Mainfray and P. Agostini, eds. (Le Commissarial à l'Energie Atomique, Paris, 1990), pp. 45–55.
5. K. C. Kulander, K. J. Schafer, and J. L. Krause, "Dynamics of short-pulse excitation, ionization and harmonic conversion," in *Super Intense Laser–Atom Physics*, B. Piraux, A. L'Huillier, and K. Rzążewski, eds., Vol. 316 of NATO ASI Series (Plenum, New York, 1993), pp. 95–110.
6. M. Lewenstein, Ph. Balcou, M. Yu. Ivanov, A. L'Huillier, and P. B. Corkum, "Theory of high harmonic generation by low frequency laser fields," Phys. Rev. A **49,** 2117–2132 (1994).
7. K. C. Kulander and B. W. Shore, "Calculations of multiple-harmonic conversion of 1064-nm radiation in Xe," Phys. Rev. Lett. **62,** 524–526 (1989).
8. K. C. Kulander and B. W. Shore, "Generation of optical harmonics by intense pulses of laser radiation. II. Single-atom spectrum for xenon," J. Opt. Soc. Am. B **7,** 502–508 (1990).
9. A. L'Huillier, K. J. Schafer, and K. C. Kulander, "Theoretical aspects of intense field harmonic generation," J. Phys. B **24,** 3315–3341 (1991).
10. A. L'Huillier, Ph. Balcou, S. Candel, K. J. Schafer, and K. C. Kulander, "Calculations of high-order harmonic-generation processes in xenon at 1064 nm," Phys. Rev. A **46,** 2778–2790 (1992).
11. J. Peatross and D. D. Meyerhofer, "Measurement of the angular distribution of high-order harmonics emitted from rare gases," in *Short Wavelength V*, Vol. 17 of OSA Proceedings Series (Optical Society of America, Washington, D.C., 1993).
12. J. Peatross and D. D. Meyerhofer, "Angular distribution of high-order harmonics emitted from rare gases at low density," Phys. Rev. A **51,** R906 (1995).
13. Ph. Balcou and A. L'Huillier, "Phase-matching effects in strong-field harmonic generation," Phys. Rev. A **47,** 1447–1459 (1993).
14. S. Augst, C. I. Moore, J. Peatross, and D. D. Meyerhofer, "Spatial distribution of high-order harmonics generated in the tunneling regime," in *Short Wavelength Coherent Radiation*, P. H. Bucksbaum and N. M. Ceglio, eds., Vol. 11 of OSA Proceedings Series (Optical Society of America, Washington, D.C., 1991), pp. 23–27.
15. J. W. G. Tisch, R. A. Smith, J. E. Muffett, M. Ciarrocca, J. P. Marangos, and M. H. R. Hutchinson, "Angularly resolved high-order harmonic generation in helium," Phys. Rev. A **49,** R28–R31 (1994).
16. P. Salieres, T. Ditmire, K. S. Budil, M. D. Perry, and A. L'Huillier, "Spatial profiles of high-order harmonics generated by a femtosecond Cr:LiSAF laser," J. Phys. B **27,** L217–L222 (1994).
17. B. W. Shore and K. C. Kulander, "Generation of optical harmonics by intense pulses of laser radiation. I. Propagation effects," J. Mod. Opt. **36,** 857–875 (1989).
18. J. D. Jackson, *Classical Electrodynamics*, 2nd ed. (Wiley, New York, 1975), p. 395, Eq. (9.19).

19. J. W. Goodman, *Introduction to Fourier Optics* (McGraw-Hill, New York, 1968), p. 61.
20. P. W. Milonni and J. H. Eberly, *Lasers* (Wiley, New York, 1988), p. 490.
21. A. L'Huillier, Ph. Balcou, and L. A. Lompre, "Coherence and resonance effects in high-order harmonic generation," Phys. Rev. Lett. **68,** 166–169 (1992).
22. X. F. Li, A. L'Huillier, M. Ferray, L. A. Lompre, and G. Mainfray, "Multiple-harmonic generation in rare gases at high laser intensity," Phys. Rev. A **39,** 5751–5761 (1989).
23. J. Peatross, J. Chaloupka, and D. D. Meyerhofer, "High-order harmonic generation with an annular laser beam," Opt. Lett. **19,** 942–944 (1994).